Non-monotonous short-time decay of the Loschmidt echo in quasi-one-dimensional systems

Arseni Goussev
Institut für Theoretische Physik, Universität Regensburg, 93040 Regensburg, Germany and
School of Mathematics, University of Bristol, University Walk, Bristol BS8 1TW, United Kingdom
(Dated: May 18, 2011)

We study the short-time stability of quantum dynamics in quasi-one-dimensional systems with respect to small localized perturbations of the potential. To this end, we address, analytically and numerically, the decay of the Loschmidt echo (LE) during times short compared to the Ehrenfest time. We find that the LE is generally a non-monotonous function of time and exhibits strongly pronounced minima and maxima at the instants of time when the corresponding classical particle traverses the perturbation region. We also show that, under general conditions, the envelope decay of the LE is well approximated by a Gaussian, and we derive explicit analytical formulas for the corresponding decay time. Finally, we demonstrate that the observed non-monotonicity of the LE decay is only pertinent to one-dimensional (and, more generally, quasi-one-dimensional systems), and that the short-time decay of the LE can be monotonous in higher number of dimensions.

PACS numbers: 03.65.-w, 03.65.Sq, 05.45.Mt

I. INTRODUCTION

Nearly a quarter of a century has passed since Peres [1] made an important advance in understanding the origin of irreversibility in quantum theory. He pioneered a framework in which dynamical instabilities were studied in terms of small external perturbations of the Hamilton operator without resorting to the classical concepts of mixing and coarse graining. In particular, Peres convincingly demonstrated that a change in the time evolution of a quantum system caused by the perturbation is largely determined by whether the system exhibits regular or chaotic behavior in the classical limit.

The quantity addressed by Peres, currently known as the *Loschmidt echo* (LE) in the quantum chaos community and the *fidelity* in the field of quantum information, is defined as [1]

$$M(t) = \left| \langle \Psi_0 | \exp(i\hat{H}_2 t/\hbar) \exp(-i\hat{H}_1 t/\hbar) | \Psi_0 \rangle \right|^2 . \quad (1)$$

It is the squared overlap of the initial state $|\Psi_0\rangle$ and the state obtained by propagating $|\Psi_0\rangle$ though time t under the original, unperturbed Hamiltonian $\hat{H}_1$, and then through time $-t$ under the perturbed Hamiltonian $\hat{H}_2$. In other words, the LE, $M(t)$, is a measure of the time-reversibility of a system's dynamics under "imperfect conditions". In an alternative interpretation, the LE characterizes the distance between two states in the Hilbert space, $|\Psi_1\rangle = \exp(-i\hat{H}_1 t/\hbar)|\Psi_0\rangle$ and $|\Psi_2\rangle = \exp(-i\hat{H}_2 t/\hbar)|\Psi_0\rangle$, both obtained from the same initial state, $|\Psi_0\rangle$, in the course of the quantum evolution through time t under two different Hamiltonians, $\hat{H}_1$ and $\hat{H}_2$ respectively. By construction, $M(0) = 1$ assuming the initial state is normalized. Typically, $M(t)$ decreases (or "decays") with increasing time, and the precise functional form of the decay is determined by the nature of the Hamiltonians $\hat{H}_1$ and $\hat{H}_2$, as well as by the initial state.

Interest to the subject of the LE revived a decade ago. This was largely due to the discovery of a perturbation independent regime [2] of the LE decay in systems that exhibit chaotic dynamics in the classical limit. In this regime, known as the Lyapunov regime, the LE decays exponentially in time, $M(t) \sim \exp(-\lambda t)$, with the decay rate λ equal to the average Lyapunov exponent of the corresponding classical system. The Lyapunov regime can be considered as a clear example of how classical chaos manifests itself in a quantum mechanical world.

Roughly speaking, for chaotic systems under the action of *global* Hamiltonian perturbations, i.e., perturbations affecting a dominant part of the system's phase space, one identifies three distinct decay regimes of the LE: the Gaussian perturbative regime [3, 4] for "weak" perturbations, the exponential Fermi-golden-rule (FGR) regime [2–5] for "moderate" perturbation strengths, and the exponential Lyapunov regime [2, 6] for "strong" perturbations. The above three regimes serve as a basis for the theory of the LE decay for global perturbation. The full theory however is much more subtle and the interested reader is referred to two comprehensive review articles, Refs. [7, 8].

The LE due to global perturbations has long been a subject of numerous experimental studies. Most notably these are experiments in nuclear magnetic resonance [9–12], quantum optics [13], cold atoms [14–18], superconductivity [19], microwave cavities [20–23], and elastodynamics [24, 25].

In recent years, Hamiltonian perturbations of a new kind, namely perturbations that are *local* in phase space, have been addressed in the context of the LE decay both theoretically and experimentally [26–30]. In a semiclassical picture, a local perturbation is concentrated in a small region of the system's phase space, so that the length of a typical trajectory between any two successive visits of the perturbation region is much larger than the system's size. In strongly chaotic systems the phase space extent

of a local perturbation can be characterized by an "escape" rate $\tau_{\rm esc}^{-1}$ defined as the rate at which trajectories of the corresponding classical system visit the perturbation region. The semiclassical analysis of the LE for times longer than the Ehrenfest time, i.e., longer than the time it takes for an initially localized wave packet to explore the available phase space, has revealed an exponential decay regime, $M(t) \sim \exp(-\kappa t)$, in which the decay rate κ is a non-monotonous function of the perturbation strength [26, 28]. In particular, for sufficiently weak perturbations the FGR regime is recovered in which κ grows quadratically with the perturbations strength. However, in the limit of strong perturbations κ saturates at a perturbation independent value $2\tau_{\rm esc}^{-1}$ corresponding to the so-called escape-rate regime. The crossover from the FGR to the escape-rate regime is non-monotonous, and κ exhibits well pronounced oscillations as a function of the perturbations strength. These oscillations have been then confirmed in numerical experiments with perturbed cat maps [29] and, more recently, in laboratory experiments with microwave cavities [30]. Finally, the limit of point-like perturbations, for which $\tau_{\rm esc} \to \infty$, was addressed in Ref. [27]. There, the LE was shown to decay algebraically with time, $M(t) \sim t^{-2}$.

The existing theory of the LE decay from local perturbations is only applicable to times long compared to the Ehrenfest time. However, in certain cases the short time decay of the echo, during which the unperturbed and perturbed quantum states can be described by localized wave packets, might be of significant importance for understanding results of laboratory experiments. For instance, in echo spectroscopy experiments with cold atoms trapped inside an optical billiard [15–17] one typically observes the echo decay for times as short as only few free flight times of the corresponding classical billiard. Such time scales can be short compared to the Ehrenfest time depending on a parameter choice. It is the objective of this paper to address the short-time decay of the LE due to local Hamiltonian perturbations. More specifically, we make the first step in this direction by performing a detailed study of the LE in one-dimensional (and, more generally, quasi-one-dimensional) systems in the presence of localized perturbations of the system's potential. We show that in such systems $M(t)$ is typically a non-monotonous function exhibiting well pronounced minima and maxima at times when the particle traverses the perturbation region. We also show that in closed systems the envelope of $M(t)$ can be well approximated by a Gaussian, $\exp\left[-(t/\tau)^2\right]$, with the decay time τ explicitly expressible in terms of system parameters. All results presented in this paper concern the LE decay in "clean" systems and imply no averaging over initial states or Hamiltonian perturbations.

The analysis presented in this paper only concerns the short-time decay of the LE in conservative quasi-one-dimensional, and therefore essentially integrable, systems. The case of the LE decay in classically chaotic systems for times shorter than the Ehrenfest time (and in the presence of global perturbations) was addressed in Ref. [31]. There, for a "typical" localized initial state Ψ_0, the LE was shown to exhibit the double-exponential initial decay, $M(t) \sim \exp(-\text{constant} \times e^{2\lambda t})$ with λ being the Lyapunov exponent.

The paper is organized as follows. In Section II we provide the analysis of the LE decay in one-dimensional systems based on full numerical solution of the time-dependent Schrödinger equation and on the thawed Gaussian approximation (TGA) in its standard and modified, average potential formulations. Details on the average potential TGA are deferred to Appendix A. Particular examples treated in Section II include a free particle (Sec. II A), particle on a ring (Sec. II B), harmonic (Sec. II C 1) and anharmonic (Sec. II C 2) oscillators. Section III demonstrates disappearance of non-monotonous features of the LE decay as a quasi-one-dimensional system is transformed into a substantially two-dimensional system. In Section IV we give a discussion of our results and make concluding remarks.

II. LOSCHMIDT ECHO IN ONE DIMENSION

A. Free particle

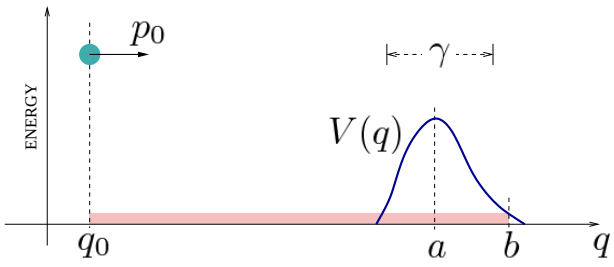

FIG. 1: (Color online) One-dimensional quantum particle in the presence of a localized potential barrier. See the text for discussion.

The essential physics of the short-time decay of the LE for local potential perturbations can already be revealed by considering the simplest physical system – a free particle. In this scenario, the unperturbed Hamiltonian, $\hat{H}_1 = \hat{p}^2/2m$, describes one-dimensional motion of a free particle of mass m; in the coordinate representation, the momentum operator $\hat{p} = -i\hbar\partial/\partial q$. The perturbed Hamiltonian, $\hat{H}_2 = \hat{H}_1 + V(\hat{q})$, represents a particle interacting with a potential "barrier" $V(q)$ localized to an interval on the position axis, see Fig. 1. For concreteness, we assume $V(q)$ to have a single maximum (or minimum) at $q = a$. (As it will become clear from the following presentation, our results can be easily generalized to perturbation potentials of arbitrary shape.) We also label the characteristic extent of the potential by γ, see Fig. 1. Finally, we set the initial state to be a

Gaussian wave packet,

$$\Psi_0(q) = \left(\frac{1}{\pi\sigma^2}\right)^{\frac{1}{4}} \exp\left(\frac{i}{\hbar}p_0(q-q_0) - \frac{(q-q_0)^2}{2\sigma^2}\right) \quad (2)$$

that represents a quantum particle with the average position coordinate q_0 and momentum p_0. The initial wave packet dispersion is quantified by σ. We further assume that the initial state, $\Psi_0(q)$, has zero overlap with the perturbation potential, i.e.,

$$\gamma, \sigma \ll l\,, \quad (3)$$

where $l = |a - q_0|$ is the characteristic distance between the particle and the perturbation region, see Fig. 1. We also assume that the initial state is well localized in the momentum space, so that

$$p_0\sigma \gg \hbar\,, \quad (4)$$

and that the potential $V(q)$ constitutes a classically small perturbation:

$$|V(q)| \ll E\,, \quad (5)$$

where $E = p_0^2/2m$ is the total energy of the corresponding classical particle. Together Eqs. (4) and (5) imply that the probability density gets almost perfectly transmitted over the barrier in the course of the time evolution, and the effect of quantum reflections can be neglected.

Most of semiclassical studies of the LE decay rely on the so-called "dephasing representation" (DR) [32, 33], in which the LE amplitude $\langle\Psi_2(t)|\Psi_1(t)\rangle$ is expressed as an interference integral over trajectories of the unperturbed system, modulated by a "dephasing" factor due to the perturbation, with initial phase space coordinates weighed by the Wigner function of the state $|\Psi_0\rangle$. Our analysis however is based on a different analytical approach, namely on the "thawed Gaussian" approximation (TGA) [34–36] in its standard and extended versions, see Appendix A and the discussion below. The TGA, unlike the DR, involves only a single trajectory transporting the wave packet center through phase space in the course of its time evolution. This allows for greater analytical flexibility at the expense of a reduction in accuracy. For most of our purposes however the TGA proves to be sufficiently reliable both qualitatively and quantitatively.

According to the TGA both the unperturbed and perturbed wave functions preserve their Gaussian form in the course of their time evolution:

$$\Psi_j(q;t) = \left(\frac{2\Re\alpha_j}{\pi}\right)^{\frac{1}{4}} \times \exp\left(-\alpha_j(q-q_j)^2 + \frac{i}{\hbar}p_j(q-q_j) + \frac{i}{\hbar}\phi_j\right), \quad (6)$$

where $j = 1, 2$ labels the unperturbed and perturbed wave functions respectively, and $\Re$ stands for the real part. Here, $q_j(t)$, $p_j(t)$, $\phi_j(t)$ are real-valued and $\alpha_j(t)$ complex-valued functions of time that parametrize the wave functions. In the "standard" TGA [34–36] the time evolution of these parameters is governed by

$$\dot{q}_j = p_j/m\,, \quad (7)$$

$$\dot{p}_j = -W_j'(q_j)\,, \quad (8)$$

$$\dot{\alpha}_j = -\frac{2i\hbar}{m}\alpha_j^2 + \frac{i}{2\hbar}W_j''(q_j)\,, \quad (9)$$

and $\dot{\phi}_j = p_j^2/2m - W_j(q_j) - (\hbar^2/m)\Re\alpha_j$. Here $W_j(q)$ is the corresponding (unperturbed for $j = 1$ and perturbed for $j = 2$) potential, and the prime denotes differentiation with respect to q. The system of four real, first order ordinary differential equations given by Eqs. (7–9) is then solved with the initial conditions $q_j = q_0$, $p_j = p_0$, and $\alpha_j^{-1} = 2\sigma^2$ at $t = 0$. In the "average potential" TGA, see Appendix A, Eqs. (7–9) are replaced by

$$\dot{q}_j = p_j/m\,, \quad (10)$$

$$\dot{p}_j = -\widetilde{W}_j'(q_j; \Re\alpha_j)\,, \quad (11)$$

$$\dot{\alpha}_j = -\frac{2i\hbar}{m}\alpha_j^2 + \frac{i}{2\hbar}\widetilde{W}_j''(q_j; \Re\alpha_j)\,, \quad (12)$$

with the average potential $\widetilde{W}_j$ defined as

$$\widetilde{W}_j(q;s) = (2s/\pi)^{\frac{1}{2}} \int dx\, W_j(x) e^{-2s(x-q)^2}. \quad (13)$$

As before the prime denotes partial differentiation with respect to q.

In the free particle case the unperturbed wave function $\Psi_1(q;t)$ given by the TGA, Eq. (6), is exact and the parameters q_1, p_1, and α_1 evolve in time according to [36]

$$q_1 = q_0 + p_0 t/m\,, \quad (14)$$

$$p_1 = p_0\,, \quad (15)$$

$$\alpha_1^{-1} = 2(\sigma^2 + i\hbar t/m)\,, \quad (16)$$

and $\phi_1 = (p_0^2/2m)\,t - (\hbar/2)\arctan(\hbar t/m\sigma^2)$.

Time evolution of the parameters q_2, p_2, α_2 characterizing the perturbed wave function $\Psi_2(q;t)$ are determined from a set of three ordinary differential equations (7–9) in the "standard TGA" and by equations (10–13) in the "average potential TGA" with $j = 2$ and $W_2(q) = V(q)$. Here we note that the LE defined by Eq. (1) is unaffected by the global phases ϕ_1 and ϕ_2 in the regime that allows one to approximate the unperturbed and perturbed states by the simple Gaussian wave packets given by Eq. (6). The phase ϕ of an individual Gaussian wave packet would only be physically relevant if the initial state Ψ_0 was a superposition of two or more Gaussian wave packets, or if one was interested in the LE amplitude $\langle\Psi_2(t)|\Psi_1(t)\rangle$ rather than in $M(t)$. However, considerations of these kinds go beyond the scope of the current study.

Substituting the two time-dependent Gaussian wave packets, given by Eq. (6) with $j = 1$ and 2, into Eq. (1) we obtain for the LE

$$M(t) = \frac{2\sqrt{\Re\alpha_1 \Re\alpha_2}}{|\alpha_1 + \alpha_2^*|} \exp\left[- \frac{2}{|\alpha_1 + \alpha_2^*|^2} \times \left(\Re\big(\alpha_1\alpha_2(\alpha_1+\alpha_2)^*\big)\Delta q^2 + \Im(\alpha_1\alpha_2)\frac{\Delta q \Delta p}{\hbar} + \Re(\alpha_1+\alpha_2)\frac{\Delta p^2}{4\hbar^2} \right) \right], \quad (17)$$

where $\Delta q = q_2 - q_1$ and $\Delta p = p_2 - p_1$, asterisk denotes complex conjugation, and $\Im$ stands for the imaginary part. Equation (17), along with equations describing time evolution of the parameters q_j, p_j, and α_j with $j = 1, 2$, provides the main framework for our analytical study of the LE.

We also perform a numerical analysis of the problem of the LE decay. To this end we adopt a method of expending the quantum propagator $\exp(-i\hat{H}t/\hbar)$ in terms of Chebyshev polynomials of the Hamiltonian $\hat{H}$. For a detailed discussion of the method see Ref. [37] and references within. Hereinafter we refer to results of the numerical solution of the LE decay problem as to "exact" results as opposed to approximate ones obtained by using the standard and average potential TGA.

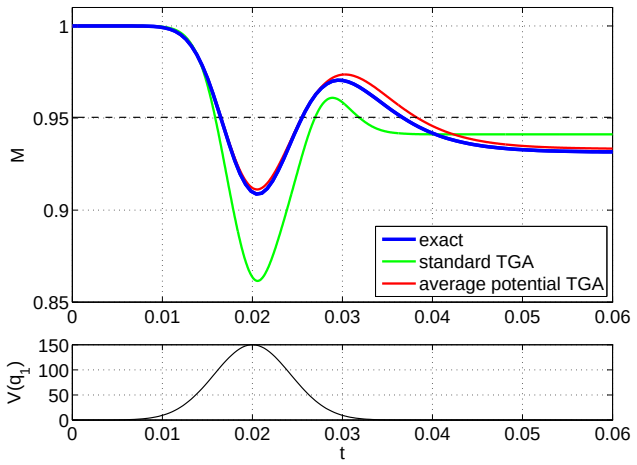

FIG. 2: (Color online) Top figure: The LE, $M(t)$, for a free particle with the perturbation potential $V(q)$ given by Eq. (18). The horizontal dashed line represents the LE saturation value $M(\infty)$ given by Eq. (28). Bottom figure: Perturbation potential as seen by the unperturbed classical particle, i.e. $V(q_1(t))$. The system is characterized by $p_0 = 50$, $\sigma = 0.1$, $a - q_0 = 1$, $\gamma = 0.3$, and $V_0 = 150$.

Figure 2 shows the LE decay for the case of a perturbation potential given by the Gaussian barrier

$$V(q) = V_0 \exp\left(-\frac{(q-a)^2}{\gamma^2} \right). \quad (18)$$

The upper part of the figure displays $M(t)$. Here, the thick blue curve shows a result of the full, quantum-mechanical computation of the LE defined by Eq. (1), i.e., the exact LE decay. The green curve is obtained by using the standard TGA, i.e., Eq. (17) with the time evolution of parameters q_2, p_2, and α_2 determined from Eqs. (7–9). The red curve represents the LE decay obtained in the average potential TGA by using Eqs. (10–13) for the time evolution of q_2, p_2, and α_2. The initial wave packet, Eq. (2), is specified by $q_0 = -1$, $p_0 = 50$, and $\sigma = 0.1$ [43]. The perturbation potential is given by Eq. (18) with $a = 0$, $\gamma = 0.3$, and $V_0 = 150$. The lower part of Fig. 2 shows the function $V(q_1(t))$, which has the meaning of the perturbation potential as "seen" by the unperturbed classical particle.

Figure 2 prompts an interesting observation: the LE develops a minimum at the time the unperturbed classical particle passes the extremum of the perturbation potential, and a maximum at the time the particle exits the perturbation region. In fact, such behavior is generic. This can be shown by imposing the approximation $\alpha_2(t) \simeq \alpha_1(t)$, which simplifies Eq. (17) to

$$M(t) = \exp\left[-\frac{1}{\Re\alpha_1} \left(|\alpha_1|^2 \Delta q^2 + \Im\alpha_1 \frac{\Delta q \Delta p}{\hbar} + \frac{\Delta p^2}{4\hbar^2} \right) \right]. \quad (19)$$

Then, substituting Eq. (16) into Eq. (19) we obtain

$$M(t) = \exp\left[-\frac{1}{2\sigma^2} \left(\Delta q - \frac{t}{m}\Delta p \right)^2 - \frac{1}{2}\left(\frac{\sigma \Delta p}{\hbar} \right)^2 \right]. \quad (20)$$

The function $M(t)$, given by Eq. (20), possesses two extrema at time instants determined by

$$\frac{d}{dt}\Delta p = 0 \qquad \text{(minimum)}, \quad (21)$$

$$\Delta q = \left[1 + \left(\frac{m\sigma^2}{\hbar t} \right)^2 \right] \frac{t}{m}\Delta p \qquad \text{(maximum)}. \quad (22)$$

We now utilize the standard TGA, Eqs. (7) and (8) with $j = 2$ and $W_2(q) = V(q)$, to express the position and momentum shifts, Δq and Δp, in terms of the perturbation $V(q)$. To the leading order in V_0/E, with $V_0 = \max_q |V(q)|$, we obtain

$$\Delta q(t) = -\frac{1}{p_0}\int_0^t dt' V(q_1(t')), \quad (23)$$

$$\Delta p(t) = -\frac{m}{p_0} V(q_1(t)). \quad (24)$$

Substitution of Eq. (24) into Eq. (21) shows that $M(t)$ exhibits a minimum at time $t_a = m(a - q_0)/p_0 = ml/|p_0|$, with a being the extremum point of the perturbation potential, see Fig. 1. It is the time instant at which the unperturbed classical particle passes the extremum point of the perturbation potential, i.e., $q_1(t_a) = a$. Similarly, the LE exhibits a maximum at time $t_b = m(b - q_0)/p_0$

that, in accordance with Eqs. (22), (23) and (24), satisfies

$$\int_0^{t_b} dt' V(q_1(t')) = \left(t_b + \frac{(m\sigma^2/\hbar)^2}{t_b} \right) V(q_1(t_b)) \,. \quad (25)$$

In the limit $t \gg m\sigma^2/\hbar$, or equivalently $l \gg p_0\sigma^2/\hbar$, Eq. (25) simplifies to

$$\int_{q_0}^{b} dq V(q) = |b - q_0| V(b) \,. \quad (26)$$

Equation (26) has a simple geometrical interpretation as depicted in Fig. 1: the area under the curve $V(q)$ from q_0 to b equals the area of a rectangle with the base $|b - q_0|$ and height $V(b)$. It is clear from this construction that the LE exhibits a maximum when the classical unperturbed particle leaves the perturbation region.

The time instant $t = t_b$, at which $M(t)$ exhibits a maximum, has the following physical significance. According to Eq. (22), and in the limit $l \gg p_0\sigma^2/\hbar$, it satisfies $\Delta q(t_b) = \Delta p(t_b) t_b/m$. This means that if the perturbed wave packet, $\Psi_2(q; t_b)$, is propagated backward through time $-t_b$ under the unperturbed (free-particle) Hamiltonian $\hat{H}_1$ then the resulting wave packet is centered at q_0. In other words, the states $|\Psi_0\rangle$ and $|e^{i\hat{H}_1 t_b/\hbar} e^{-i\hat{H}_2 t_b/\hbar} |\Psi_0\rangle$ have the same expectation values of the position operator (while generally different expectation values of the momentum operator).

Finally, at long times, $t \gg ml/p_0$, one has $\Delta q = -(m/p_0^2) \int_{-\infty}^{+\infty} dq V(q)$ and $\Delta p = 0$. Thus, in accordance with Eq. (20), the LE saturates at the value

$$M(\infty) = \exp\left[-\frac{1}{8} \left(\frac{1}{\sigma E} \int_{-\infty}^{+\infty} dq V(q) \right)^2 \right] . \quad (27)$$

For the case of a perturbation potential given by Eq. (18) the saturation value is

$$M(\infty) = \exp\left[-(\pi/8)(\gamma/\sigma)^2 (V_0/E)^2 \right] . \quad (28)$$

In Fig. 2 the LE saturation value, $M(\infty)$, calculated in accordance with Eq. (28) is shown by a horizontal dashed line. We note that the quantitative agreement between the LE saturation value obtained by numerically solving the Schrödinger equation and the saturation value given by Eqs. (27) and (28) improves as the perturbation strength V_0 is reduced. This is consistent with the fact that Eqs. (27) and (28) are valid only in the leading order of V_0/E.

As it will become clear from the following sections the observed non-monotonicity of $M(t)$ is a generic feature of the LE decay in one-dimensional (and, more generally, quasi-one-dimensional) systems. We now turn our attention to closed systems and address the envelope of $M(t)$. The analysis presented here is valid for short times, for which the wave function stays localized and can be well approximated by a Gaussian wave packet. In other words, we restrict our discussion to $t \ll t_E$ with t_E being the Ehrenfest time.

B. Particle on a ring

As the fist example of a closed one-dimensional system we consider a quantum particle moving on a ring. In this set-up the wave function of the unperturbed system, $\Psi_1(q; t)$, is defined on an interval $0 \le q \le L$, and satisfies the time-dependent Schrödinger equation with the Hamiltonian $\hat{H}_1 = \hat{p}^2/2m$ and periodic boundary condition $\Psi_1(L; t) = \Psi_1(0; t)$. The Hamiltonian of the perturbed system is $\hat{H}_2 = \hat{H}_1 + V(q)$, where $V(q)$ is defined on the same q-interval with $V(L) = V(0)$. As before, we assume $V(q)$ to be localized in a small region of size γ around a single extremum point a, see Fig. 1. The wave function of the perturbed system, $\Psi_2(q; t)$, satisfies the same periodic boundary conditions, $\Psi_2(L; t) = \Psi_2(0; t)$. Finally, as in Section II A, we assume the validity of conditions given by Eqs. (3–5).

As stated above, we only consider the wave packet dynamics for times shorter than the Ehrenfest time, $t \ll t_E$. The latter is the time that it takes for the wave packet dispersion, initially equal to σ, to become comparable to the size of the system, L. (We note, that Eq. (3) implies $\sigma \ll L$.) According to the uncertainty principle the velocity uncertainty of the particle is $\Delta v \sim \hbar/m\sigma$. Thus, for the case of the free motion on a ring, the Ehrenfest time can be estimated as $t_E \sim L/\Delta v \sim m\sigma L/\hbar$.

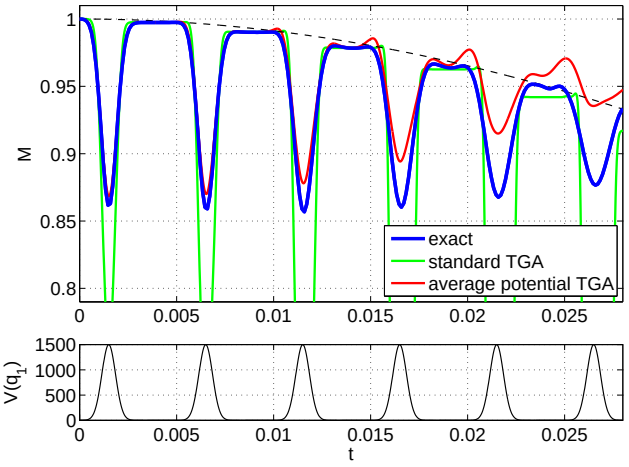

FIG. 3: (Color online) Top figure: The LE, $M(t)$, for a particle on a ring with the perturbation potential $V(q)$ given by Eq. (18). The dashed line represents the envelope decay, $\overline{M}(t)$, calculated in accordance with Eqs. (29) and (31). Bottom figure: Perturbation potential as seen by the unperturbed particle, i.e. $V(q_1(t))$. The system is characterized by $L = 1$, $p_0 = 200$, $\sigma = 0.1$, $a - q_0 = 0.3$, $\gamma = 0.1$, and $V_0 = 1500$.

Since the dispersion of the wave packet and the extent of the perturbation potential are small compared to the ring circumference L, the problem in question is effectively equivalent to that of a free unbounded motion in the presence of a periodic perturbation potential $\sum_{n=-\infty}^{+\infty} V(q + nL)$. Therefore, according to Section II A, we expect the LE curve to exhibit a sequence of minima

at times $t_{\min,k} = m(a-q_0+kL)/p_0$, with $k \in \mathbb{N}_0$, at which the unperturbed classical particle traveling a constant velocity p_0/m passes the extrema of the periodic perturbation potential. (For concreteness but without loss of generality, we consider the case $0 < q_0 < a < L$ and $p_0 > 0$.) Indeed, such a non-monotonous time decay of the LE is found in perfect agreement with the results of the fully numerical (exact) and semianalytical (TGA) solutions of the problem, see Fig. 3. We also note here that, just as in Fig. 2, $M(t)$ in Fig. 3 exhibits a sequence of local maxima at times $t^+_{\max,k} \simeq m(a-q_0+\gamma+kL)/p_0$ and $t^-_{\max,k+1} \simeq m\big(a-q_0-\gamma+(k+1)L\big)/p_0$, with $k \in \mathbb{N}_0$. These time instants are solutions of Eq. (25) for t_b with $V(q)$ replaced by the periodic potential $\sum_{n=-\infty}^{+\infty} V(q+nL)$.

In order to find the envelope function $\overline{M}(t)$ of the LE decay curve we consider M at times $t_n = nT$, where $n \in \mathbb{N}$, and $T = mL/p_0$ is the period of the unperturbed motion. According to Eqs. (20) and (23) we have $M(t_n) = \exp(-\Delta q^2/2\sigma^2)$ with $\Delta q = -(t_n/p_0L)\int_0^L dqV(q)$. This leads to

$$\overline{M}(t) = \exp\left[-(t/\tau)^2\right] \tag{29}$$

with $\tau = \tau_{\rm ring}$ and

$$\tau_{\rm ring} = \sqrt{2}|p_0|\sigma L \left|\int_0^L dqV(q)\right|^{-1}. \tag{30}$$

For the case of a Gaussian perturbation potential given by Eq. (18) the expression for the decay time reduces to

$$\tau_{\rm ring} = T\sqrt{\frac{8}{\pi}\frac{\sigma E}{\gamma|V_0|}}\,, \tag{31}$$

where $E = p_0^2/2m$ is the total energy of the system.

The dashed curve in Fig. 3 is the envelope function $\overline{M}(t)$ calculated from Eqs. (29) and (31) for the system specified by $L = 1$, $p_0 = 200$, $\sigma = 0.1$, $a - q_0 = 0.3$, $\gamma = 0.1$, and $V_0 = 1500$. It is evident that $\overline{M}(t)$ accurately describes the envelope of the exact LE decay represented by the thick blue curve. It is also interesting to compare the quality of the approximate solutions. The standard TGA (green curve) reasonably well approximates $M(t)$ around its maxima, while completely failing to capture the function close to its minima. On the other hand, the average potential TGA (red curve) well describes both maxima and minima. This approximation however turns out to be only limited to short times, up to 3 full cycles of the particle around the ring for the particular set of parameters, after which the approximation becomes unstable.

C. Particle in a well

We now consider a quantum particle trapped inside a one-dimensional potential well, so that $\hat{H}_1 = \hat{p}^2/2m + U(\hat{q})$ and $\hat{H}_2 = \hat{p}^2/2m + U(\hat{q}) + V(\hat{q})$, where $U(q)$ specifies the potential well, and $V(q)$ represents a perturbation potential localized around $q = a$. As before, we assume validity of the conditions given by Eqs. (3–5) with the total energy of the classical particle $E = p_0^2/2m + U(q_0)$. We also assume $E > U(a) + V(a)$, so that both unperturbed and perturbed classical motions have the same turning points q_- and q_+, see Fig. 4.

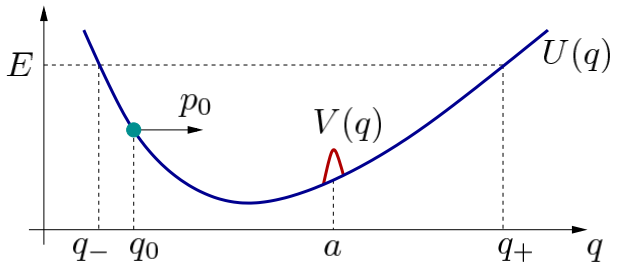

FIG. 4: (Color online) A quantum particle in a one-dimensional potential well. The unperturbed potential is given by $U(q)$, and the perturbed potential by $U(q) + V(q)$. The total energy E of the system is such that both unperturbed and perturbed classical motions have the same turning points q_- and q_+.

As we will see below the LE decay for the system under consideration is non-monotonous. Deep local mimima surrounded by (generally less pronounced) local maxima occur when the classical unperturbed particle traverses the perturbation region. The physics underlying this non-monotonicity is essentially the same as in the cases of a free particle and a particle on a ring, see Sections II A and II B, so we directly proceed to the analysis of the envelope function $\overline{M}(t)$ of the LE decay $M(t)$.

We begin by considering the period $T + \Delta T$ of the classical oscillatory motion of the perturbed system:

$$\begin{aligned} T + \Delta T &= \sqrt{2m}\int_{q_-}^{q_+} \frac{dq}{\sqrt{E - U(q) - V(q)}} \\ &\simeq T + \sqrt{\frac{m}{2}}\int_{q_-}^{q_+} dq\, V(q)\big(E - U(q)\big)^{-\frac{3}{2}}, \end{aligned} \tag{32}$$

where

$$T = \sqrt{2m}\int_{q_-}^{q_+} \frac{dq}{\sqrt{E - U(q)}} \tag{33}$$

is the period the unperturbed classical motion. Equation (32) holds to the second order in $V/(E-U)$. Then, assuming that $\big(E - U(q)\big)$ is approximately constant in a γ-interval about $q = a$, we obtain

$$\Delta T = \sqrt{\frac{m}{2}}\big(E - U(a)\big)^{-\frac{3}{2}}\int_{-\infty}^{+\infty} dqV(q)\,. \tag{34}$$

Here we note that if the perturbation potential satisfies $\int dqV(q) = 0$ then the expansion in Eq. (32) has to be terminated at the next order resulting in $\Delta T \sim \int dqV^2(q)$.

The envelope function $\overline{M}(t)$ of the LE decay curve can be calculated using the approximation given by Eq. (19). To this end we consider the distance between the unperturbed and perturbed trajectories in phase space, $\Delta q = q_2 - q_1$ and $\Delta p = p_2 - p_1$, at times $t_n = nT$ with $n \in \mathbb{N}$. Since T is the period of the unperturbed systems we have $q_1(t_n) = q_0$ and $p_1(t_n) = p_0$. The trajectory of the perturbed system however is "delayed" by the time $n\Delta T$ with respect to the unperturbed trajectory. This, for small ΔT, can be written as $q_2(t_n) = q_1(t_n - n\Delta T)$ and $p_2(t_n) = p_1(t_n - n\Delta T)$. Expanding these equations to the leading order in $\Delta T/T$ we obtain

$$\Delta q(t_n) = -\frac{p_0}{m}\frac{\Delta T}{T}t_n\,, \tag{35}$$

$$\Delta p(t_n) = U'(q_0)\frac{\Delta T}{T}t_n\,, \tag{36}$$

where the prime denotes the derivative. Then, a substitution of Eqs. (35) and (36) into Eq. (19) yields

$$M(t_n) = \exp\left[-\chi(t_n)\left(\frac{\Delta T}{T}t_n\right)^2\right] \tag{37}$$

with

$$\chi = \frac{1}{\Re\alpha_1}\left[\left(|\alpha_1|\frac{p_1}{m}\right)^2 - \Im\alpha_1\frac{p_1U'(q_1)}{m\hbar} + \left(\frac{U'(q_1)}{2\hbar}\right)^2\right], \tag{38}$$

keeping in mind that $q_1 = q_1(t)$, $p_1 = p_1(t)$, $\alpha_1 = \alpha_1(t)$, and $q_1(t_n) = q_0$, $p_1(t_n) = p_0$.

It is now interesting to observe that χ is a constant of the motion defined by Eqs. (7–9) with $j = 1$ and $W_1(q) = U(q)$. Indeed, it is straightforward to verify that

$$\frac{d\chi}{dt} = 0\,. \tag{39}$$

Then, a replacement of $\chi(t_n)$ in Eq. (37) by its value at time $t = 0$,

$$\chi = \frac{1}{2}\left(\frac{p_0}{m\sigma}\right)^2 + \frac{1}{2}\left(\frac{\sigma U'(q_0)}{\hbar}\right)^2, \tag{40}$$

yields the Gaussian LE envelope $\overline{M}(t)$ given by Eq. (29) with the decay time $\tau = \tau_{\rm well}$ and

$$\tau_{\rm well} = \frac{T}{\Delta T}\chi^{-\frac{1}{2}} = \sqrt{2}\frac{T}{\Delta T}\left[\left(\frac{p_0}{m\sigma}\right)^2 + \left(\frac{\sigma U'(q_0)}{\hbar}\right)^2\right]^{-\frac{1}{2}}. \tag{41}$$

Below we consider some particular potentials $U(q)$ and compare the analytical prediction given by Eq. (41) with the numerical, full quantum-mechanical solution of the LE decay problem.

1. *Harmonic oscillator*

As our first example we considering motion of a particle in a harmonic potential well for which $U(q) = m\omega^2q^2/2$. In this case the time evolution of the unperturbed system is governed by [36]

$$q_1 = q_0\cos\omega t + \frac{p_0}{m\omega}\sin\omega t\,, \tag{42}$$

$$p_1 = p_0\cos\omega t - m\omega q_0\sin\omega t\,, \tag{43}$$

$$\alpha_1 = \left(\frac{m\omega}{2\hbar}\right)\frac{\hbar\cos\omega t + im\omega\sigma^2\sin\omega t}{i\hbar\sin\omega t + m\omega\sigma^2\cos\omega t}\,. \tag{44}$$

Equations (6) and (42–44) give the exact quantum dynamics of the system with the Hamiltonian $\hat{H}_1$ and initial state of Eq. (2). As before, the time dependent parameters q_2, p_2, and α_2 characterizing the perturbed wave packet are calculated using the standard TGA, Eqs. (7–9), or the average potential TGA, Eqs. (10–13), with $W_2(q) = U(q) + V(q)$. Then, the TGA approximation of the LE is computed from Eq. (17), and the envelope function, $\overline{M}(t)$, from Eqs. (29) and (41) with $T = 2\pi/\omega$ and ΔT given by Eq. (34).

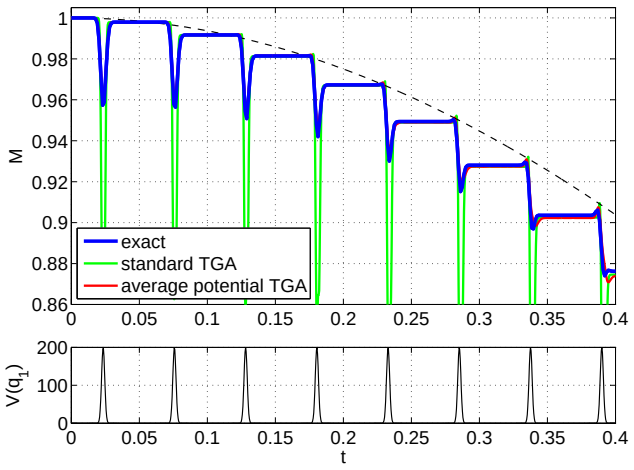

FIG. 5: (Color online) Top figure: the LE, $M(t)$, for a particle in a parabolic well with the perturbation potential $V(q)$ given by Eq. (18). The dashed line represents the envelope decay, $\overline{M}(t)$, calculated in accordance with Eqs. (29) and (41). Bottom figure: the perturbation potential as seen by the unperturbed particle, i.e. $V(q_1(t))$. The system is characterized by $\omega = 60$, $q_0 = -1$, $p_0 = 10$, $\sigma = 0.1$, $a = 0$, $\gamma = 0.1$, and $V_0 = 200$. Note that the LE decay obtained by the average potential TGA (red curve) is essentially indistinguishable from the exact result (blue thick curve) for most of the time range.

Figure 5 shows the time decay of the LE for a quantum particle in the harmonic potential well. The unperturbed system is defined by $\omega = 60$, $q_0 = -1$, $p_0 = 10$, $\sigma = 0.1$. The perturbation potential is given by Eq. (18) with $a = 0$, $\gamma = 0.1$, and $V_0 = 200$. As before, the thick blue curve represents $M(t)$ obtained by numerically solving the time dependent Schrödinger equation for the perturbed system. (The exact time evolution of the unperturbed system is given by Eqs. (6) and (42–44).) The green curve corresponds to the standard TGA for the perturbed system, i.e., Eqs. (7–9) with

$W_2(q) = m\omega^2 q^2/2 + V(q)$. It is clear from the figure that the standard TGA fails to reproduce the minima of the exact LE curve. On the other hand, the average potential TGA result, computed according to Eqs. (10–13) and represented by the red curve, provides an excellent approximation of the exact result. The dashed line shows the envelope decay, $\overline{M}(t)$, predicted by Eqs. (29) and (41). A reasonable agreement between the theoretical and numerical results is apparent.

2. *Anharmonic oscillator*

We now consider, as our unperturbed system, a quantum particle moving in an anharmonic potential well of the form $U(q) = m\omega^2 q^2/2 + \epsilon q^3$. Here, the computational procedure of the LE decay is essentially the same as in Section II C 1 with the only difference that the oscillation period T is obtained by numerically evaluating the integral in Eq. (33).

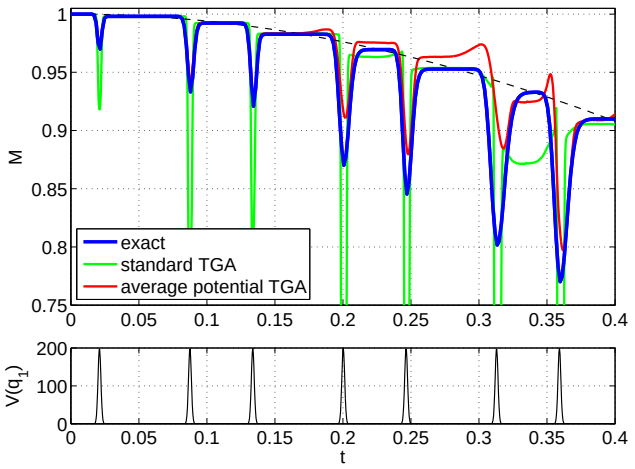

FIG. 6: (Color online) Top figure: the LE, $M(t)$, for a particle in an anharmonic well with the perturbation potential $V(q)$ given by Eq. (18). The dashed line represents the envelope decay, $\overline{M}(t)$, calculated in accordance with Eqs. (29) and (41). Bottom figure: the perturbation potential as seen by the unperturbed particle, i.e. $V(q_1(t))$. The system is characterized by $\omega = 60$, $\epsilon = -400$, $q_0 = -1$, $p_0 = 10$, $\sigma = 0.1$, $a = 0$, $\gamma = 0.1$, and $V_0 = 200$.

Figure 6 shows the time decay of the LE for a quantum particle in the anharmonic potential well. The unperturbed system is defined by $\omega = 60$, $\epsilon = -400$, $q_0 = -1$, $p_0 = 10$, $\sigma = 0.1$. The perturbation potential is given by Eq. (18) with $a = 0$, $\gamma = 0.1$, and $V_0 = 200$. The thick blue curve represents the exact LE decay. The green curve corresponds to the standard TGA for the unperturbed and perturbed systems, i.e., Eqs. (7–9) with $W_1(q) = U(q)$ and $W_2(q) = U(q) + V(q)$. Once again, the standard TGA fails to reproduce the minima of the exact LE curve. The red curve shows the result of the average potential TGA, i.e., Eqs. (10–13) with $W_1(q) = U(q)$ and $W_2(q) = U(q) + V(q)$. It well approximates the exact LE decay curve for up to two full oscillations of the unperturbed system. The dashed line shows the envelope decay, $\overline{M}(t)$, predicted by Eqs. (29) and (41). As in Section II C 1, one observes a reasonable agreement between the theoretical and numerical results.

III. BEYOND ONE DIMENSION

In this section we argue that the reported non-monotonicity of the short-time decay of the LE is pertinent mainly to one-dimensional (or, more generally, quasi-one-dimensional) systems. The disappearance of the non-monotonicity of the LE decay in systems with two or higher number of dimensions can be understood as follows. In one-dimensional systems an initially Gaussian wave packet traverses the perturbation region and approximately preserves its Gaussian shape provided the strength of the perturbation potential is small compared to the energy of the particle. In this case the TGA provides a natural basis for the LE analysis and the theory developed in Section II holds. In higher number of dimensions however it is often energetically preferable for the wave packet to split in parts and circumvent the perturbation region. The wave packet deforms to avoid the perturbation region and can no longer be approximated by a Gaussian. The overlap between the unperturbed (approximately Gaussian) and perturbed (substantially non-Gaussian) wave packets decays rapidly and monotonically during the time that the system interacts with the perturbation.

To illustrate this point we consider the time decay of the LE for a free quantum particle in two dimensions under the action of a Gaussian perturbation potential. The initial state of the particle is given by

$$\Psi_0(x,y) = \frac{1}{\sqrt{\pi}\sigma} \exp\left(\frac{i}{\hbar} p_0 (x - x_0) - \frac{(x-x_0)^2 + (y-y_0)^2}{2\sigma^2} \right). \quad (45)$$

Here, (x_0, y_0) is the center of the wave packet, p_0 the magnitude of the momentum pointing along the x-axis, and σ its dispersion. The perturbation potential is defined as

$$V(x,y) = V_0 \exp\left(-\frac{(x-a)^2}{\gamma^2} - \frac{y^2}{\delta^2} \right) \quad (46)$$

with γ and δ quantifying the extent of the perturbation region in the x- and y-directions respectively. As in Section II we assume the validity of the conditions given by Eqs. (3–5).

Figure 7 shows the time decay of the LE, $M(t)$, obtained by numerically solving the time-dependent Schrödinger equation with the initial state given by Eq. (45) and the Hamiltonian operators $\hat{H}_1 = (-\hbar^2/2m)(\partial^2/\partial x^2 + \partial^2/\partial y^2)$ and $\hat{H}_2 = \hat{H}_1 + V(\hat{x}, \hat{y})$,

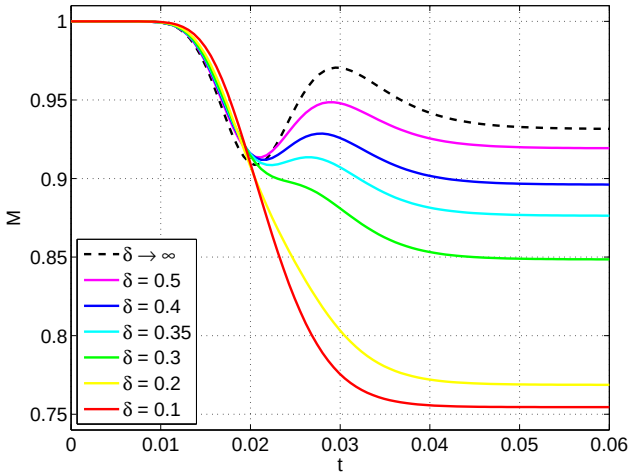

FIG. 7: (Color online) The LE decay for a free particle in two dimensions under the action of the perturbation potential given by Eq. (46). The system is characterized by $p_0 = 50$, $\sigma = 0.1$, $a - q_0 = 1$, $V_0 = 150$, and $\gamma = 0.3$. The $M(t)$ curves correspond to seven different values of the y-extent of the perturbation region: from bottom to top $\delta = 0.1$, 0.2, 0.3, 0.35, 0.4, 0.5, and ∞.

where $V(x, y)$ is defined by Eq. (46). The system parameters are $p_0 = 50$, $\sigma = 0.1$, $a - q_0 = 1$, $V_0 = 150$, and $\gamma = 0.3$. Six different values of the y-axis extent of the perturbation region are considered, $\delta = 0.1$, 0.2, 0.3, 0.35, 0.4, 0.5, as well as the case $\delta \to \infty$ corresponding to the one-dimensional problem analyzed in Section II A. It is clear from the figure that in quasi-one-dimensional systems, i.e., when $\sigma \ll \delta$ so that the y-component of the classical force exerted on the particle by the perturbation potential is negligible, $M(t)$ exhibits minima and maxima as the particle traverses the perturbation region. On the other hand, in substantially two-dimensional systems, i.e., for $\delta \lesssim \sigma$, a fast monotonous decay of the LE is observed.

In order to support our qualitative explanation for the disappearance of the non-monotonicity in the LE decay for small values of δ we depict in Fig. 8 the time evolution of the unperturbed and perturbed wave functions for the system characterized by $p_0 = 50$, $\sigma = 0.1$, $a - q_0 = 1$, $V_0 = 150$, $\gamma = 0.3$, $\delta = 0.1$. This set of parameters corresponds to the LE decay represented by the red (most bottom) curve in Fig. 7. Here, a snapshot at the top shows the probability distribution of the initial state. The left column shows the probability distribution of the unperturbed wave packet at regular time intervals. The corresponding snapshots in the right column give the probability distribution of the perturbed wave function. A white ellipse in the right column shows the characteristic extent of the perturbation potential: the ellipse is centered at the maximum of the Gaussian potential, and its major and minor semi-axes equal to $\gamma = 0.3$ and $\delta = 0.1$ respectively. The figure demonstrates how the probability distribution of the perturbed wave function changes

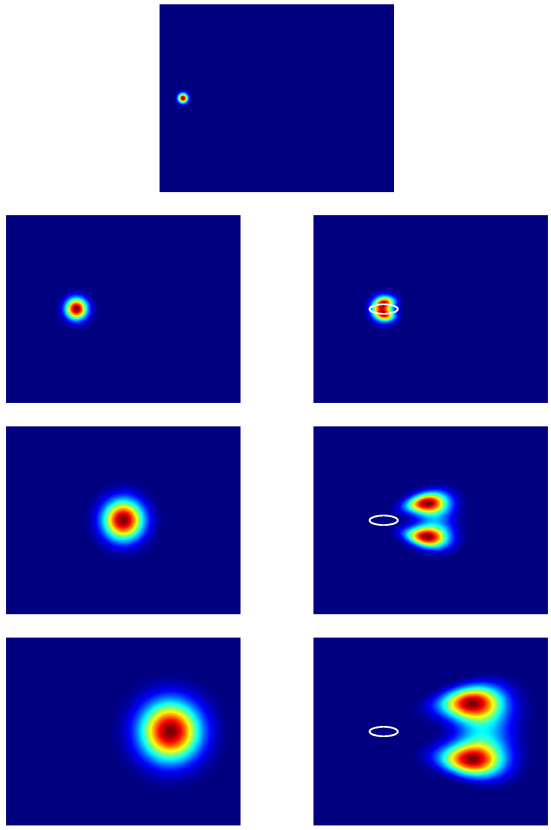

FIG. 8: (Color online) The time evolution of the unperturbed (left column) and perturbed (right column) wave function. The top snapshot shows the initial state. The white ellipse in the snapshots of the right column is centered at the position of the perturbation maximum, and has its major and minor semi-axes equal to $\gamma = 0.3$ and $\delta = 0.1$ respectively. The system is characterized by $p_0 = 50$, $\sigma = 0.1$, $a - q_0 = 1$, $V_0 = 150$, $\gamma = 0.3$, $\delta = 0.1$, and exhibits a LE decay represented by the red (most bottom) curve in Fig. 7.

from a simple Gaussian to a double-peak function as the quantum particle circumvents the perturbation region. Clearly, this process can not be adequately described by the TGA. It is also natural to expect the LE overlap to decay monotonically and faster than in the limit of large δ, in which the perturbed wave function does not significantly change its functional form and only gets displaced in phase space with respect to the unperturbed wave packet.

The qualitative change of the LE decay shown in Fig. 7 can be linked to an effective decrease of the Ehrenfest time t_E of the perturbed systems as the perturbation size δ decreases: the observed splitting of the wave packet indicates that $t_E \sim m(a - q_0)/p_0$ for small values of δ.

It is interesting to note that the phenomenon of wave packet splitting is observed already for relatively weak perturbation potentials. For example, the right column in Fig. 8 corresponds to the energy of the classical particle, $p_0^2/2$, being more than 8 times higher than the

strength of the potential, V_0. At this point, it is not clear whether the splitting can be adequately explained in terms of deflection of the corresponding classical trajectories or whether quantum interference effects play a crucial role. It can be speculated that the wave packet splitting is intimately related to the phenomenon of coherent electron flow branching in two-dimensional quantum wells with weak disordered background potentials [38–40]. However, a proper investigation is yet to be performed.

As a final remark we make the following counter-intuitive observation. By increasing the parameter δ, while keeping V_0 fixed, one increases the overall presence of the perturbation, in the sense that the integral $\int dxdy\, V(x,y)$ becomes larger. However, at the same time, the larger δ the higher the LE saturation value, see Fig 7, and therefore the smaller the effect of the perturbation on the time evolution of the wave function. The reason for that is that it is energetically preferable for a wave function to avoid small perturbation regions by changing its shape. This results in small values of the LE overlap. On the other hand, spatially extended perturbation regions are traversed by the wave function without any significant shape change resulting in large values of the LE overlap.

IV. CONCLUSIONS

We have studied, analytically and numerically, the decay of the Loschmidt echo (LE) from local Hamiltonian perturbations for times short compared to the Ehrenfest time. During those times the quantum states of the unperturbed and perturbed systems can be efficiently approximated by localized Gaussian wave packets. The latter evolve in accordance with equations of the thawed Gaussian approximation (TGA). We have analyzed these equations and deduced several important properties of the LE decay in quasi-one-dimensional systems.

Firstly, we have shown that the LE is generally a non-monotonous function of time. More specifically, $M(t)$ exhibits strongly pronounced minima and maxima at the instants of time when the corresponding classical particle traverses the perturbation region. The minima of $M(t)$ are reached when the particle passes the peak (or bottom) of the perturbation potential, whereas the maxima generally occur at the times the particle enters or exits the perturbation region. We have also demonstrated that while the observed non-monotonicity of the LE decay is generic in one-dimensional systems the short-time decay can be monotonous in systems with higher number of dimensions.

Secondly, using the TGA we have analyzed the envelope decay of the LE and shown it to be well approximated by a Gaussian, $\overline{M}(t) = \exp\left[-(t/\tau)^2\right]$. The decay time τ is expressible in terms of parameters of the initial state, system's Hamiltonian, and perturbation potential. We have given explicit formulas for the cases of a particle on a ring, Eq. (30), and a particle inside a smooth potential well of an arbitrary shape, Eq. (41). The analytical formulas have been given convincing numerical support.

All results presented in this paper pertain to the short-time decay of the LE in "clean" quantum systems and assume no averaging over initial states or Hamiltonian perturbations. In this respect, the findings may prove valuable in echo experiments which imply no or minimal averaging intrinsically. Thus, for example, in echo experiments with ultra-cold atoms one could try to use an experimentally observed decay function $M(t)$ to reconstruct the localized perturbation potential.

Acknowledgments

This work in its early stage was supported by EPSRC under Grant No. EP/E024629/1. The author would like to thank Philippe Jacquod and Klaus Richter for reading and helping to improve the manuscript.

Appendix A: Thawed Gaussian approximations

The celebrated thawed Gaussian approximation (TGA), originally introduced by Heller [34], is a semiclassical technique for propagation of localized Gaussian wave packets in time without having to solve the full Schrödinger equation. The approximation is based on the idea that, at least for short times, the expectation values of the position and momentum operators, q_j and p_j respectively, evolve according to the classical, Hamilton equations of motion. Thus, in the TGA the evolving wave packet is "guided" by a single real phase-space trajectory described by the Hamilton equations. The TGA is one of the simplest approximations to the full Van Vleck-Gutzwiller semiclassical propagator [41].

Below we begin with a brief discussion of the standard TGA following Ref. [34]. A comprehensive review of the subject can be found in Ref. [35]. We then introduce an extended version of the approximation – the average potential TGA – that proves more reliable for potentials with rapid spatial variations.

The central assumption of the TGA is that an initially Gaussian wave packet preserves its Gaussian form, $\Psi_j(q;t)$ as given by Eq. (6), throughout the time evolution under a Hamiltonian $\hat{H}_j = \hat{p}^2/2m + W_j(\hat{q})$. The wave packet is parametrized by one complex-valued – $\alpha_j(t)$ – and three real-valued – $q_j(t)$, $p_j(t)$, and $\phi_j(t)$ – functions, which are determined by substituting Ψ_j into the

Schrödinger equation:

$$\left[\left(i\hbar\dot{\alpha}_j - \frac{2\hbar^2}{m}\alpha_j^2\right)(q-q_j)^2 + \dot{p}_j(q-q_j) - 2i\hbar\alpha_j\left(\dot{q}_j - \frac{p_j}{m}\right)(q-q_j) + \dot{\phi}_j - p_j\dot{q}_j + \frac{p_j^2}{2m} + W_j(q) + \frac{\hbar^2}{m}\alpha_j - \frac{i\hbar}{4}\frac{\Re\dot{\alpha}_j}{\Re\alpha_j}\right]\Psi_j(q;t) = 0\,. \quad \text{(A1)}$$

Here dots represent differentiation with respect to time. Clearly, Eq. (A1) can not be satisfied for a general potential $W_j(q)$. However, an approximate solution of Eq. (A1) can be found by expanding the potential $W_j(q)$ into the power series about $q = q_j$ to the second order in $(q - q_j)$, and then separately comparing terms of the same order. This procedure yields Eqs. (7–9) together with $\dot{\phi}_j = p_j^2/2m - W_j(q_j) - (\hbar^2/m)\Re\alpha_j$.

The standard TGA, Eqs. (7–9), relies on the quadratic approximation of the potential $W_j(q)$ about $q = q_j$, and is therefore limited to potentials varying slowly on the scale given by the spatial extent of the wave packet. In order to lift this limitation we modify the TGA method as discussed below.

The problem of finding the "best" functions $\alpha_j(t)$, $q_j(t)$, $p_j(t)$, and $\phi_j(t)$ approximating the time evolution of the wave packet allows for an alternative approach. If $\Psi_j(q;t)$, given by Eq. (6), were a true solution of the time-dependent Schrödinger equation with the Hamiltonian $\hat{H}_j = \hat{p}^2/2m + W_j(\hat{q})$ then the expectation value of any (generally time-dependent) operator $\hat{O}_j$ would satisfy

$$\frac{d}{dt}\langle\Psi_j|\hat{O}_j|\Psi_j\rangle = \frac{i}{\hbar}\langle\Psi_j|[\hat{H}_j,\hat{O}_j]|\Psi_j\rangle + \langle\Psi_j|\frac{\partial\hat{O}_j}{\partial t}|\Psi_j\rangle \quad \text{(A2)}$$

with $[\cdot,\cdot]$ denoting the commutator. For a general potential W_j, however, $\Psi_j(q;t)$ given by Eq. (6) is not a true solution of the Schrödinger equation, and, therefore, Eq. (A2) can only be satisfied by four linearly independent Hermitian operators $\hat{O}_j$. A choice of these four operators uniquely defines the functions $\alpha_j(t)$, $q_j(t)$, and $p_j(t)$. (Equation (A2) is unaffected by the global phase ϕ_j. This phase however is of no importance to the problem of the Loschmidt echo decay addressed in this paper.) Although there is no unique choice of the four independent Hermitian operators $\hat{O}_j$ we proceed with the seemingly most natural ones: $\hat{q}$, $\hat{p}$, $\hat{q}^2$, and $\hat{p}^2$. Straightforward calculations yield Eqs. (10–13) for the time evolution of q_j, p_j, and α_j. Obviously, the requirement that $\Psi_j(q;t)$ satisfies Eq. (A2) for $\hat{O}_j = \hat{q},\ \hat{p},\ \hat{q}^2,\ \hat{p}^2$ guaranties the resulting approximation, which we here term the average potential TGA, to predict the phase space dynamics of the wave packet's center and dispersion in the best possible way.

Here two final remarks are in order. Firstly, since $\widetilde{W}_j'(q_j;\Re\alpha_j) = \langle\Psi_j|W_j'(\hat{q})|\Psi_j\rangle$ Eqs. (10) and (11) are nothing but the statement of the Ehrenfest theorem [36]. Secondly, it can be readily shown that in the case of the potential $W_j(q)$ being a second order polynomial in q Eqs. (7–9) are identical with Eqs. (10–12). In this case $\Psi_j(q;t)$ constitutes the true solution of the Schrödinger equation.

The idea of exploiting average potentials for propagation of Gaussian wave packets has been previously discussed in the chemical physics literature, e.g., see Ref. [42]. These approaches however deal with potentials averaged with respect to Gaussian wave functions with "frozen" exponents (such as $\Psi_j(q;t)$ in Eq. (6) with $\alpha_j(t) = \alpha_0$) and are generally different from the average potential TGA presented above. It would be interesting to compare these different methods in terms of their precision and computational efficiency.

[1] A. Peres, Phys. Rev. A **30**, 1610 (1984).
[2] R. A. Jalabert and H. M. Pastawski, Phys. Rev. Lett. **86**, 2490 (2001).
[3] P. Jacquod, P. G. Silvestrov, and C. W. J. Beenakker, Phys. Rev. E **64**, 055203(R) (2001).
[4] N. R. Cerruti and S. Tomsovic, Phys. Rev. Lett. **88**, 054103 (2002).
[5] T. Prosen, Phys. Rev. E **65**, 036208 (2002).
[6] F. M. Cucchietti, C. H. Lewenkopf, E. R. Mucciolo, H. M. Pastawski, and R. O. Vallejos, Phys. Rev. E **65**, 046209 (2002).
[7] T. Gorin, T. Prosen, T. H. Seligman, and M. Znidaric, Phys. Rep. **435**, 33 (2006).
[8] P. Jacquod and C. Petitjean, Adv. Phys. **58**, 67 (2009).
[9] E. L. Hahn, Phys. Rev. **80**, 580 (1950).
[10] S. Zhang, B. H. Meier, and R. R. Ernst, Phys. Rev. Lett. **69**, 2149 (1992).
[11] G. Usaj, H. M. Pastawski, and P. R. Levstein, Mol. Phys. **95**, 1229 (1998).
[12] H. M. Pastawski, P. R. Levstein, G. Usaj, J. Raya, and J. Hirschinger, Physica A **283**, 166 (2000).
[13] N. A. Kurnit, I. D. Abella, and S. R. Hartmann, Phys. Rev. Lett. **13**, 567 (1964).
[14] F. B. J. Buchkremer, R. Dumke, H. Levsen, G. Birkl, and W. Ertmer, Phys. Rev. Lett. **85**, 3121 (2000).
[15] M. F. Andersen, A. Kaplan, and N. Davidson, Phys. Rev. Lett. **90**, 023001 (2003).
[16] M. F. Andersen, T. Grünzweig, A. Kaplan, and N. Davidson, Phys. Rev. A **69**, 063413 (2004).
[17] M. F. Andersen, A. Kaplan, T. Grünzweig, and N. Davidson, Phys. Rev. Lett. **97**, 104102 (2006).
[18] S. Wu, A. Tonyushkin, and M. G. Prentiss, Phys. Rev. Lett. **103**, 034101 (2009).
[19] Y. Nakamura, Y. A. Pashkin, T. Yamamoto, and J. S. Tsai, Phys. Rev. Lett. **88**, 047901 (2002).
[20] R. Schäfer, H.-J. Stöckmann, T. Gorin, and T. H. Selig-

man, Phys. Rev. Lett. **95**, 184102 (2005).
[21] R. Schäfer, T. Gorin, T. H. Seligman, and H.-J. Stöckmann, New J. Phys. **7**, 152 (2005).
[22] J. D. Bodyfelt, M. C. Zheng, T. Kottos, U. Kuhl, and H.-J. Stöckmann, Phys. Rev. Lett. **102**, 253901 (2009).
[23] B. Köber, U. Kuhl, H.-J. Stöckmann, T. Gorin, D. V. Savin, and T. H. Seligman, Phys. Rev. E **82**, 036207 (2010).
[24] T. Gorin, T. H. Seligman, and R. L. Weaver, Phys. Rev. E **73**, 015202(R) (2006).
[25] O. I. Lobkis and R. L. Weaver, Phys. Rev. E **78**, 066212 (2008).
[26] A. Goussev and K. Richter, Phys. Rev. E **75**, 015201(R) (2007).
[27] R. Höhmann, U. Kuhl, and H.-J. Stöckmann, Phys. Rev. Lett. **100**, 124101 (2008).
[28] A. Goussev, D. Waltner, K. Richter, and R. A. Jalabert, New J. Phys. **10**, 093010 (2008).
[29] N. Ares and D. A. Wisniacki, Phys. Rev. E **80**, 046216 (2009).
[30] B. Köber, U. Kuhl, H. Stöckmann, A. Goussev, and K. Richter, Phys. Rev. E **83**, 016214 (2011).
[31] P. G. Silvestrov, J. Tworzydlo, and C. W. J. Beenakker, Phys. Rev. E **67**, 025204(R) (2003).
[32] J. Vaníček, Phys. Rev. E **70**, 055201(R) (2004).
[33] J. Vaníček, Phys. Rev. E **73**, 046204 (2006).
[34] E. J. Heller, J. Chem. Phys. **62**, 1544 (1975).
[35] E. J. Heller, Acc. Chem. Res. **39**, 127 (2006).
[36] D. J. Tannor, *Introduction to Quantum Mechanics: A Time Dependent Perspective* (University Science Books, Sausalito, 2007).
[37] H. De Raedt, J. S. Kole, K. F. L. Michielsen, and M. T. Figge, Comp. Phys. Comm. **156**, 43 (2003).
[38] M. A. Topinka, B. J. LeRoy, R. M. Westervelt, S. E. J. Shaw, R. Fleischmann, E. J. Heller, K. D. Maranowski, and A. C. Gossard, Nature **410**, 183 (2001).
[39] M. A. Topinka, R. M. Westervelt, and E. J. Heller, Phys. Today **56** (12), 47 (2003).
[40] J. Vaníček and E. J. Heller, Phys. Rev. E **67**, 016211 (2003).
[41] M. C. Gutzwiller, *Chaos in Classical and Quantum Mechanics* (Springer, New York, 1990).
[42] M. S. Child, P. Sherratt, and Y. K. Sturdy, J. Phys. Chem. A **108**, 8860 (2004).
[43] Dimensionless (atomic) units, $\hbar = m = 1$, are used in all numerical examples throughout the paper.